Applied Science, Computing and Energy, 2026, 4(6), 960-981

Phytochemical and Elemental Characterization of Eleusine coracana Seed Extract for Preliminary Evaluation of Its Radioprotective Potential

Fatima Habib Sadauki*, Fatima Salmanu Koki and Fatima Tijjani Shehu

Received: 29 May 2026/Accepted: 20 August 2026/ Published: 24 August 2026

Abstract: *The study investigated the phytochemical and elemental characteristics of an aqueous extract of Eleusine coracana seeds using Fourier Transform Infrared (FTIR) spectroscopy and Neutron Activation Analysis (NAA). The work was undertaken as an initial characterization component of a broader radio protective investigation. NAA revealed a mineral-rich elemental profile, with potassium (K) being the most abundant detected element at 15460 ± 62 mg/kg, followed by rubidium (Rb) at 364 ± 9 mg/kg, sodium (Na) at 219 ± 1 mg/kg, bromine (Br) at 38.4 ± 0.2 mg/kg, zinc (Zn) at 55 ± 4.29 mg/kg, barium (Ba) at 23.9 ± 5.7 mg/kg, and iron (Fe) at 33 mg/kg. Several trace elements, including La, Sm, Sc, Co, Cs, Eu, Tb and Th, were also detected, while As, U and Sb were below the detection limit. FTIR analysis showed characteristic absorption bands between 3160.8 and 663.5 cm^{-1}, indicating molecular groups associated with O–H/N–H, C–H, amide, carboxylate, phospholipid, carbohydrate and aromatic structures. The most prominent absorbance values included 0.373 at 1576.7 cm^{-1} and 0.380 at 1039.9 cm^{-1}. A theoretical background based on electromagnetic photon energy, molecular vibrational absorption and the Beer–Lambert law is presented to provide a physics-based framework for interpreting the spectral data. The combined NAA and FTIR findings demonstrate that the extract contains nutritionally relevant elements and diverse functional groups that may contribute to its biological activity and warrant further investigation of its radio protective potential.*

Keywords: *Eleusine coracana; FTIR spectroscopy; Neutron Activation Analysis; phytochemicals; elemental composition; radioprotection.*

Fatima Habib Sadauki *
Department of Physics, Bayero University Kano, Nigeria.
Email: xahraahabeeb97@gmail.com
https://orcid.org/0009-0009-1681-0984
***Corresponding Author**

Fatima Salmanu Koki
Department of Physics, Bayero University Kano, Nigeria.
Email: Fskoki.phy@buk.edu.ng

Fatima Tijjani Shehu
Department of Physics, Ahmadu Bello University, Zaria, Nigeria.
Email: shehufatimatijjani663@gmail.com

1.0 Introduction

Ionizing radiation poses significant risks across industrial, medical and energy sectors, including applications in X-ray systems, nuclear power, food sterilization and research facilities (Bagheri et al., 2018; Chai et al., 2020). Prolonged exposure can produce biological effects ranging from molecular and cellular damage to tissue injury, genetic alterations and carcinogenesis (Desouky et al., 2015; Stone et al., 2003). Unlike non-ionizing environmental energy such as heat, ionizing radiation carries sufficient energy to produce ionization and excitation, initiating chemical changes in biological matter. The magnitude of radiation-induced effects depends on radiation type and energy, absorbed dose, exposure time, dose distribution and shielding conditions (ICRP, 1991; Tekin et al., 2018). These potential health hazards have increased the need for effective radioprotective agents

capable of reducing radiation-induced cellular and molecular damage without producing significant adverse effects

The search for naturally derived radio protective agents has attracted attention because radiation-induced oxidative stress can initiate molecular damage through reactive species. Although synthetic radio protectors such as amifostine are available, limitations associated with cost, administration and adverse effects encourage investigation of plant-derived alternatives. Although synthetic radioprotective agents such as amifostine have demonstrated protective activity, their clinical application may be limited by high cost, administration-related challenges, and undesirable side effects. These limitations have encouraged the search for safer, affordable, and naturally derived. Natural products containing antioxidant and bioactive constituents may provide useful candidates for further radiobiological investigation. Plant materials are particularly attractive because they contain diverse bioactive constituents, including phenolics, flavonoids, vitamins, and essential minerals, which may act individually or synergistically against radiation-induced oxidative stress

The mechanisms by which natural products may confer radioprotection are multifaceted. Ionizing radiation induces oxidative stress primarily through the radiolysis of water, generating reactive oxygen species (ROS) such as hydroxyl radicals (•OH), superoxide anions ($O_2^{\bullet -}$), and hydrogen peroxide (H_2O_2). These species attack cellular macromolecules including DNA, proteins, and membrane lipids (Desouky et al., 2015; Dowlath et al., 2021). The radioprotective activity of natural products may therefore involve the direct scavenging of reactive oxygen species, enhancement of endogenous antioxidant defence systems, inhibition of lipid peroxidation, protection of cellular membranes, and regulation of DNA repair and apoptosis (Arzoo *et* al., 2024; Ibrahim *et al*., 2024; Kokisi, *et al*., 2026). (Jagetia, 2007; Montoro et al., 2023). However, the presence of antioxidant constituents in a plant extract does not automatically establish radioprotective efficacy, since the actual protective effect depends on the concentration, bioavailability, interactions, and biological activity of the constituent compounds

Among plant resources with potential health-promoting properties, Eleusine coracana (finger millet or ragi) is an important cereal crop cultivated in parts of South Asia and eastern and southern Africa. It is nutritionally rich in carbohydrates, dietary fiber, proteins, amino acids and minerals, and contains phenolic and flavonoid constituents (Fuller, 2014; Ramashia et al., 2019; Hassan et al., 2021). These constituents make the plant of interest in studies of antioxidant activity and possible protection against oxidative damage.

Eleusine coracana contains phenolic compounds, flavonoids, and other phytochemicals that exhibit antioxidant properties (Hassan et al., 2021; Ramashia et al., 2019). Phenolic and flavonoid compounds may contribute to antioxidant protection through hydrogen- or electron-donation mechanisms, metal-ion interactions, and the neutralization of reactive oxygen speciesFurthermore, the mineral content—particularly zinc, iron, and selenium—plays essential roles as cofactors for antioxidant enzymes. Zinc is a structural component of Cu/Zn-superoxide dismutase, while iron is required for catalase activity (Prasad, 2013; Underwood, 1977). Elements such as zinc and iron are also biologically important because they participate in antioxidant-related enzymes and cellular metabolic processes. Nevertheless, their presence in an extract does not necessarily indicate their bioavailability, chemical form, or direct contribution to antioxidant or radioprotective activityPrevious investigations have largely emphasized the nutritional, antioxidant, and functional-food properties of finger millet, whereas its chemical characteristics in relation to possible

radioprotective applications remain comparatively less explored. The coexistence of phytochemical-related functional groups and nutritionally relevant elements may provide a chemical basis for further investigation; however, biological and radiobiological experiments are required to confirm whether the extract produces measurable radioprotective effects.

A preliminary assessment of the chemical constituents of plant extracts requires complementary analytical techniques capable of providing information about both molecular functional groups and elemental composition. Fourier-transform infrared spectroscopy (FTIR) is useful for identifying characteristic absorption bands associated with functional groups such as hydroxyl, carbonyl, amine, and aromatic structures. These bands can provide preliminary evidence of phytochemical-related molecular features, although FTIR alone cannot conclusively identify individual compounds or establish their concentrations Absorption at characteristic wavenumbers corresponds to molecular vibrations and provides a spectral fingerprint of the chemical constituents present in a sample (Nandiyanto et al., 2019). Neutron activation analysis (NAA) provides information on the elemental composition of the extract by measuring characteristic gamma rays emitted by radionuclides formed during neutron irradiation. The technique is useful for detecting and quantifying selected elements, but it does not directly determine their chemical speciation, bioavailability, or biological functionThe two methods are therefore complementary: FTIR provides molecular-functional information, whereas NAA provides elemental information. The combined use of FTIR and NAA therefore provides complementary information on the molecular-functional and elemental characteristics of the extract and may help establish a basis for subsequent phytochemical and radiobiological investigations.

Although the nutritional and phytochemical properties of Eleusine coracana have been documented, limited attention has been given to the combined assessment of the functional-group characteristics and elemental composition of its seed extract in relation to potential radioprotective applications. In particular, the chemical information obtained from FTIR and NAA has not been sufficiently integrated to provide a preliminary compositional basis for further radioprotective investigations. This study therefore addresses the need for baseline molecular-functional and elemental information before biological tests of the extract are undertaken.

The significance of this study lies in providing preliminary information on the chemical characteristics of E. coracana seed extract. The findings may support the identification of functional groups and elements potentially associated with antioxidant-related activity and may provide useful baseline data for subsequent in vitro, in vivo, and radiobiological studies. The study is intended as a chemical characterization investigation and does not, by itself, establish the radioprotective efficacy of the extract.

The aim of this study was to assess the functional-group and elemental composition of Eleusine coracana seed extract as a preliminary investigation of its potential radioprotective properties. Specifically, the study sought to identify the major FTIR absorption bands and their associated functional groups and to determine the elemental composition of the extract using neutron activation analysis. The results are expected to provide chemical evidence for further investigation but should not be interpreted as direct proof of radioprotective activity in the absence of biological or radiobiological validation.

The present paper focuses specifically on the extraction and analytical characterization of Eleusine coracana seed extract. It is intended as an initial publication component of a broader investigation into the potential radio protective

properties of the plant. The objectives were to determine the elemental composition of the aqueous extract using NAA and to identify its major infrared absorption bands and associated functional groups using FTIR spectroscopy. A theoretical framework is included to establish the physical basis of the spectroscopic measurements and the interpretation of absorbance.

1.1 Theoretical Background Neutron Activation Analysis (NAA)

Neutron activation analysis (NAA) is a nuclear analytical technique based on the irradiation of a sample with neutrons to produce radioactive nuclides that subsequently decay by emitting characteristic gamma rays. . For a neutron-capture reaction, a target nucleus absorbs a neutron and forms an excited compound nucleus. The excited nucleus then releases excess energy, commonly through prompt gamma-ray emission, to form a radioactive product nuclideWhen a sample is irradiated in a nuclear reactor, thermal neutrons undergo capture reactions with target nuclei according to

$$^{A}_{Z}X + ^{1}_{0}n \rightarrow ^{A+1}_{Z}X^{*} \rightarrow ^{A+1}_{Z}X + \gamma \qquad (1)$$

The activated radionuclide subsequently undergoes radioactive decay and emits gamma rays with energies characteristic of the radionuclide. These gamma-ray energies are used for qualitative identification, while the measured peak areas are used for quantitative determination

$$^{A+1}_{Z}X \rightarrow ^{A+1}_{Z+1}Y + \beta^{-} + \bar{\nu}_{e} + \gamma \qquad (2)$$

Assuming a constant neutron flux, negligible depletion of the target isotope, and production through a single neutron-capture reaction, the activity of the radionuclide at the end of irradiation is expressed as equation 3

$$A_0 = N\sigma\phi(1 - e^{-i\lambda t}) \qquad (3)$$

where A_0 is the activity at the end of irradiation (Bq), N is the number of target atoms, σ is the neutron capture cross-section (cm^2), ϕ is the neutron flux (n cm^{-2} s^{-1}), λ is the radioactive decay constant (s^{-1}), t_i is the irradiation time (s), and e is the exponential constant (2.718)

The term $(1 - e^{-i\lambda t})$ is referred to as the saturation factor and accounts for the simultaneous production and decay of radionuclides during irradiation (De Soete *et al*., 1972). For short irradiation times relative to the radionuclide half-life, the saturation factor is small, whereas it approaches unity as the irradiation time becomes sufficiently long compared with the radionuclide half-life

The mass of an element in the sample can be determined by comparing the gamma-ray peak area of the sample with that of a standard reference material:

$$m_x = m_{std}\left(\frac{C_x}{C_{std}}\right)\left(\frac{D_{std}}{D_x}\right)\left(\frac{F_{std}}{F_x}\right) \qquad (4)$$

where C represents net peak area, *D* accounts for decay corrections, and *F* includes correction factors for irradiation, counting geometry, and detector efficiency. The correction factors may account for differences in irradiation conditions, decay time, counting time, detector efficiency, counting geometry, neutron flux, and sample–standard configuration, depending on the analytical procedure used

Key advantages of NAA include: (a) high sensitivity for many elements (ppm to ppb levels), (b) multi-elemental capability, (c) minimal sample preparation, and (d) freedom from reagent contamination. The technique is particularly suitable for biological samples because it can detect trace elements that may be metabolically significant (Ehmann & Vance, 1991; Glascock, 2004). Nevertheless, the sensitivity of NAA depends on the neutron flux, irradiation and decay periods, detector efficiency, nuclear cross-section, radionuclide half-life, and the presence of interfering gamma-ray peaks.

The principal nuclear reactions, radionuclide half-lives, and characteristic gamma-ray energies considered for the identification of the elements investigated in this study are presented in Table 1

Table 1. Nuclear parameters for elements determined by NAA

Element	Nuclear Reaction	Half-life	γ-ray Energy (keV)
Na	$^{23}Na(n,\gamma)^{24}Na$	15.0 h	1368.6
K	$^{41}K(n,\gamma)^{42}K$	12.36 h	1524.7
Br	$^{79}Br(n,\gamma)^{80}Br$	17.7 min	617.1
Zn	$^{64}Zn(n,\gamma)^{65}Zn$	244.3 d	1115.5
Fe	$^{58}Fe(n,\gamma)^{59}Fe$	44.5 d	1099.2, 1291.6
Co	$^{59}Co(n,\gamma)^{60}Co$	5.27 y	1173.2, 1332.5
Ba	$^{130}Ba(n,\gamma)^{131}Ba$	11.5 d	496.3
Rb	$^{85}Rb(n,\gamma)^{86}Rb$	18.6 d	1076.6
Cs	$^{133}Cs(n,\gamma)^{134}Cs$	2.06 y	795.8
Sc	$^{45}Sc(n,\gamma)^{46}Sc$	83.8 d	889.3, 1120.5
La	$^{139}La(n,\gamma)^{140}La$	40.3 h	1596.2
Sm	$^{152}Sm(n,\gamma)^{153}Sm$	46.5 h	103.2
Eu	$^{151}Eu(n,\gamma)^{152}Eu$	13.5 y	1408.0
Th	$^{232}Th(n,\gamma)^{233}Th \rightarrow ^{233}Pa$	27.0 d	311.9

Fourier Transform Infrared (FTIR) spectroscopy is based on the interaction of infrared electromagnetic radiation with molecular vibrational modes. The energy of infrared radiation is related to its frequency and wavelength by the Planck relationship:

$$E = h\nu = \frac{hc}{\lambda} = hc\tilde{\nu} \quad (5)$$

where E is the photon energy, h is Planck's constant, c is the speed of light, λ is the wavelength, and $\tilde{\nu}$is the wavenumber. In FTIR spectroscopy, wavenumber (cm^{-1}) is used to represent the position of absorption bands and is directly related to the vibrational energy of molecular bonds. The vibrational wavenumber of a bond can be approximated using the harmonic oscillator model:

$$\tilde{\nu} = \frac{1}{2\pi c}\sqrt{\frac{k}{\mu}} \quad (6)$$

where $k$is the bond force constant and $\mu$is the reduced mass of the bonded atoms. Thus, different molecular bonds and functional groups exhibit characteristic infrared absorption bands.

The intensity of infrared absorption is commonly described by the Beer–Lambert relationship:

$$A = \varepsilon bc \quad (7)$$

where A is absorbance, ε is the molar absorptivity, $b$is the optical path length, and $c$is the concentration of the absorbing species. Absorbance may also be expressed as $A = \log_{10}(I_0/I)$, where I_0 and I represent the incident and transmitted radiation intensities, respectively. In the present study, absorbance values are used primarily to compare the relative prominence of the observed FTIR bands, while the corresponding wavenumbers are used for functional-group interpretation. This provides the physical basis for relating the spectral features of *Eleusine coracana* seed extract to its molecular composition.

FTIR spectroscopy and NAA provide complementary information about biological extracts. While FTIR identifies molecular functional groups through vibrational spectroscopy—revealing the presence of proteins, lipids, carbohydrates, and aromatic compounds—NAA determines the elemental composition at trace levels. Together, these techniques offer a comprehensive chemical characterization: FTIR establishes the molecular environment in which elements are bound, while NAA quantifies the elemental

inventory. This combination is particularly valuable for investigating potential radio protective agents, as both the molecular antioxidants (e.g., phenolic compounds detected by FTIR) and essential trace elements (e.g., Zn, Se, detected by NAA) may contribute to radiation protection mechanisms.

2.0 Materials and Methods

2.1 Materials

Eleusine coracana seeds, distilled water, grinding machine, polyethylene sample bags, cheesecloth, centrifuge, analytical balance, FTIR spectrometer, NAA irradiation facility, HPGe gamma-ray detector and associated laboratory materials were used for the study.

2.1 Preparation of Eleusine coracana Seed Extract

The seeds were collected, washed, dried and ground into powder using a grinding machine. The powder was stored in polyethylene bags until extraction. Water was used as the extraction solvent. Fifty grams (50 g) of the powdered seed material was extracted in 1.5 L of water overnight (approximately 16 hours) at room temperature (25 ± 2 °C) with continuous stirring at 300 rpm using a magnetic stirrer. The mixture was filtered through double-folded cheesecloth and centrifuged at 4 °C for 10 min at 4000 rpm. The filtrate was subsequently concentrated under reduced pressure using a rotary evaporator at 40 °C and refrigerated at 4 °C until analysis.

2.2 FTIR Spectroscopy

The functional groups in the Eleusine coracana seed extract were investigated using FTIR spectroscopy. A small portion of the dried extract was finely ground and analyzed using an attenuated total reflectance (ATR) accessory. The analysis was performed using an Agilent Cary-300 series FTIR spectrometer. The sample was scanned over the mid-infrared region of 400–4000 cm^{-1}. Thirty-two scans were recorded and averaged at 4 cm^{-1} resolution to improve signal-to-noise ratio. A background spectrum was obtained before sample acquisition and subtracted automatically. The resulting absorption bands were assigned by comparison with established functional-group regions and the instrument/library information available for the analysis.

2.3 Neutron Activation Analysis (NAA)

2.3.1 Sample Preparation

The prepared aqueous extract was dried at 40 °C for 24 hours and packaged in pre-cleaned polyethylene vials prior to irradiation. Approximately 100 mg of dried sample was accurately weighed and sealed in polyethylene bags. Standards of known elemental composition were prepared similarly for comparative analysis. All irradiations were conducted in accordance with institutional radiation safety protocols. Sample handling, preparation, and gamma-ray measurements followed established procedures to minimize radiation exposure to personnel and ensure compliance with regulatory requirements.

2.3.2 Neutron Irradiation

The prepared sample was irradiated in a nuclear reactor under a controlled thermal-neutron flux of approximately 5×10^{11} n cm^{-2} s^{-1}. Stable nuclei present in the sample captured neutrons and were transformed into radioactive activation products. The irradiation time was optimized for each element of interest, with a typical irradiation period of 6 hours.

2.3.3 Cooling Period

Following irradiation, the sample was allowed to cool for 1 h to permit short-lived radionuclides to decay and to reduce background interference during gamma-ray measurement.

Following irradiation, the sample was allowed to cool for 1 h to permit short-lived radionuclides to decay and to reduce background interference during gamma-ray measurement.

2.3.4 Gamma-Ray Measurement

The activated sample was measured using high-resolution gamma-ray spectrometry equipped with a high-purity germanium (HPGe) detector. The detector had a relative efficiency of 20% and an energy resolution of 1.8 keV at 1332 keV (^{60}Co). Characteristic gamma-ray energies were used for radionuclide and elemental identification.

2.3.5 Elemental Identification and Quantification

Elemental identification was performed by matching measured gamma-ray energies with reference data. Quantification was based on the corresponding gamma-ray peak areas and calibration procedures using certified reference materials, with corrections for irradiation time, decay time, counting time, detector efficiency and neutron-flux parameters. Detection limits were calculated using the Currie criterion (Currie, 1968).

3.0 Results and Discussion

3.1 NAA Elemental Profile of Eleusine coracana Seed Extract

The neutron activation analysis (NAA) results revealed that the aqueous seed extract of Eleusine coracana contained a broad range of major, minor and trace elements. The elemental profile was dominated by potassium (K), followed by rubidium (Rb) and sodium (Na). Potassium was detected at 15,460±62 mg/kg, while rubidium and sodium were present at 364±9 and 219±1 mg/kg, respectively. Other relatively abundant elements included zinc (Zn), iron (Fe), bromine (Br) and barium (Ba), with concentrations of 4.2955±4.29, 333±3, 0.238.4±0.2 and 23.9±5.7 mg/kg, respectively. Chromium was detected at 1.78±0.121.78 \pm 0.121.78±0.12 mg/kg. The remaining elements occurred at substantially lower concentrations, while arsenic (As), uranium (U) and antimony (Sb) were below their respective detection limits. The complete elemental composition and detection limits are presented in Table 1. The high potassium concentration indicates that potassium was the principal mineral constituent detected in the extract. Potassium is an important intracellular cation involved in the maintenance of osmotic balance, membrane potential, acid–base regulation and cellular excitability. Sodium performs complementary functions in extracellular fluid balance, nerve transmission and transport processes across biological membranes. However, the detection of potassium and sodium in a plant extract should not be interpreted as direct evidence of membrane protection against ionizing radiation. Their physiological relevance depends on the amount consumed, absorption, distribution, chemical form and the biological condition of the exposed organism.

Table 1. Elemental composition of Eleusine coracana seed extract determined by NAA (BDL = Below Detection Limit_

Element	Concentration (mg/kg)	Detection Limit (mg/kg)
Na	219 ± 1	0.5
K	15460 ± 62	50
As	BDL	0.1
Br	38.4 ± 0.2	0.05
La	0.30 ± 0.02	0.01
Sm	0.027 ± 0.003	0.005
U	BDL	0.02
Sc	0.025 ± 0.006	0.005
Cr	1.78 ± 0.12	0.1
Fe	33 ± 3	5
Co	0.26 ± 0.03	0.02
Zn	55 ± 4.29	0.5
Rb	364 ± 9	1
Sb	BDL	0.05
Cs	0.034 ± 0.005	0.01
Ba	23.9 ± 5.7	1
Eu	0.044 ± 0.008	0.005
Tb	0.008 ± 0.002	0.002
Th	0.013 ± 0.003	0.005

Rubidium was the second most abundant detected element. Because rubidium can behave similarly to potassium in some biological transport processes, its presence may reflect the mineral composition of the plant material and the ability of the extraction procedure to recover alkali-metal constituents. Nevertheless, the biological significance of the measured rubidium concentration cannot be established from NAA alone. Similarly, the presence of bromine and barium provides

additional information about the mineral composition of the extract but does not, by itself, demonstrate a beneficial or radioprotective function.

The detected zinc concentration of 55±4.29 mg/kg is noteworthy because zinc is an essential micronutrient involved in numerous structural, catalytic and regulatory processes. Zinc contributes to the structure and function of several proteins and enzymes, including Cu/Zn-superoxide dismutase (SOD1), which participates in the cellular response to oxidative stress (Prasad, 2013). Zinc is also involved in cellular signalling, protein stabilization and the function of some DNA-associated proteins (Hambidge, 2000; Shils et al., 2006). However, the presence of zinc in the extract does not establish that the extract increases SOD activity, enhances DNA repair or protects cells from radiation-induced injury. Such effects would require direct biochemical or biological assays.

Iron was detected at 33±333 mg/kg. Iron is essential for oxygen transport, electron transfer and the activity of several enzymes. It is also associated with catalase and certain peroxidase systems. Nevertheless, iron has a dual biological character because redox-active iron can participate in Fenton-type reactions that generate highly reactive hydroxyl radicals from hydrogen peroxide. Consequently, the biological effect of iron depends on its concentration, oxidation state, chemical coordination and regulation within the biological system (Underwood, 1977). The measured iron concentration therefore indicates the presence of an essential mineral but cannot be used to infer enhanced catalase or peroxidase activity. In addition, NAA does not determine the chemical form, oxidation state or bioavailability of the detected iron.

Chromium was detected at 1.78±0.12 mg/kg, while cobalt, lanthanum, samarium, scandium, caesium, europium, terbium and thorium occurred at low concentrations. These findings demonstrate the complex mineral composition of the seed extract. However, the detection of these elements should be interpreted descriptively. Their presence does not establish that they contribute to antioxidant activity or radioprotection. In particular, the biological relevance and safety of some trace and rare-earth-associated elements require further assessment before any physiological interpretation can be made.

Arsenic, uranium and antimony were below the detection limits of 0.10.10.1, 0.020.020.02 and 0.050.050.05 mg/kg, respectively. This result indicates that these elements were not detected at or above the analytical sensitivity achieved under the experimental conditions. It should not be interpreted as proof of their complete absence. The detection limits and analytical uncertainty should be considered when comparing the present findings with other plant-based materials.

The low detection limits reported in Table 1 demonstrate the sensitivity of NAA for the characterization of elemental constituents in biological materials. NAA is particularly useful because it can detect several elements simultaneously and does not necessarily require extensive chemical digestion before analysis. The method therefore provides a valuable overview of the inorganic constituents of *E. coracana* seed extract. Nevertheless, NAA does not provide information about the molecular structures of organic constituents, their bioavailability or their biological activity. Consequently, the elemental results should be integrated with complementary techniques such as FTIR, chromatography, antioxidant assays and cellular studies.

The presence of zinc and iron is relevant to the discussion of possible radioprotective activity because both elements are associated with biological systems involved in oxidative-stress regulation. Radiation exposure can generate reactive oxygen species, including superoxide and hydroxyl radicals, through the radiolysis of water and secondary cellular reactions. Zinc is associated with the structure and function of

Cu/Zn-SOD, whereas iron is involved in several essential metabolic enzymes (Prasad, 2013; Underwood, 1977). However, the present NAA data provide only a chemical basis for further investigation. They do not demonstrate that the extract scavenges radiation-induced radicals, activates antioxidant enzymes or prevents radiation-induced cellular damage.

3.2 FTIR Profile of the Extract

Fourier-transform infrared (FTIR) spectroscopy was used to investigate the functional-group characteristics of the aqueous *E. coracana* seed extract. The spectrum displayed absorption bands between approximately 3160.8 and 663.5 cm^{-1}, indicating the presence of several molecular environments. The FTIR spectrum provides a chemical fingerprint of the extract and complements the elemental information obtained through NAA. The FTIR absorption spectrum is shown in Fig. 1.

The identified absorption bands and their tentative functional-group interpretations are summarized in Table 2. Because several functional groups may absorb within overlapping spectral regions, the assignments should be regarded as indicative rather than definitive. FTIR spectroscopy is particularly useful for identifying broad chemical classes, but it cannot independently establish the identity or concentration of specific proteins, phenolic compounds, phospholipids or polysaccharides.

3.2.1 Protein- and Peptide-Associated Bands

The absorption band at 1576.7 cm^{-1}, with an absorbance of 0.373, occurs in a region commonly associated with amide-II vibrations. Such vibrations may involve N–H bending coupled with C–N stretching. The band at 1312.0 cm^{-1}, with an absorbance of 0.239, occurs in a region that may contain amide-III-type and other overlapping vibrations. The combined presence of these bands is compatible with protein- or peptide-related molecular structures in the extract.

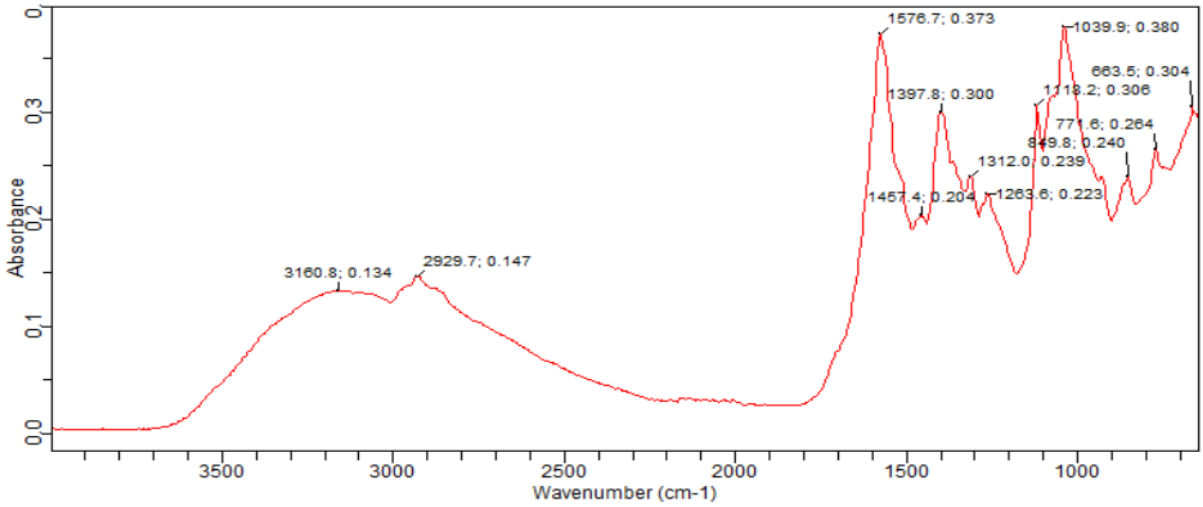

Fig. 1: FTIR absorption spectrum of Eleusine coracana seed extract in the 4000–400 cm^{-1} region, showing the principal absorption bands and their corresponding wavenumbers

Table 2. FTIR peak assignments and tentative biomolecular interpretation of the extract

Peak (cm^{-1})	Absorbance	Functional group/region	Likely vibration	Tentative biomolecular interpretation
3160.8	0.134	O–H/N–H region	Hydrogen-bonded stretching	Hydroxyl- or amino-containing constituents
2929.7	0.147	Aliphatic C–H stretch	–CH2_22/–CH3_33 stretching	Lipid- or aliphatic-chain-associated structures
1576.7	0.373	Amide-II-associated region	N–H bending and C–N stretching	Protein- or peptide-related structures
1457.4	0.204	CH2_22 bending region	Methylene deformation	Lipid-associated or other aliphatic structures
1397.8	0.300	Carboxylate-associated region	Possible COO^- symmetric stretching	Organic acids, amino-acid or carboxyl-containing structures
1312.0	0.239	Amide-III-associated region	C–N stretching and related vibrations	Protein- or peptide-related structures
1263.6	0.223	C–O/P–O^- associated region	Overlapping C–O, P–O or related vibrations	Possible ester-, phosphate- or other oxygen-containing structures
1118.2	0.304	C–O stretching region	C–O stretching	Carbohydrate, alcohol or ether-containing structures
1039.9	0.380	C–O stretching region	C–O stretching and ring-related vibrations	Strong contribution from carbohydrate-associated structures
849.8	0.240	Fingerprint region	Aromatic C–H bending or related vibration	Possible aromatic constituents
771.6	0.264	Fingerprint region	Aromatic C–H out-of-plane bending	Possible aromatic or other fingerprint-region structures
663.5	0.304	Fingerprint region	Complex skeletal or overlapping vibration	Complex structural contribution

The relatively high absorbance of the band at 1576.7 cm^{-1} indicates a strong spectral contribution under the measurement conditions. However, absorbance intensity alone cannot be used to determine the protein concentration because the measured signal depends on concentration, path length, molar absorptivity, sample preparation and matrix effects. Furthermore, the two bands do not independently identify a particular protein or peptide. The results therefore suggest the presence of nitrogen-containing and protein-related structures rather than providing conclusive molecular identification. The possible detection of protein-related structures is consistent with the known nutritional composition of finger millet, which contains proteins in addition to carbohydrates and minerals (Ramashia et al., 2019). Nevertheless, confirmation of protein content would require complementary methods such as the Kjeldahl, Bradford, Lowry or bicinchoninic acid assay.

Protein profiling could also be performed using electrophoresis or mass spectrometry.

3.2.2 Lipid-Associated Bands

The absorption band at 2929.7 cm^{-1}, with an absorbance of 0.147, is consistent with aliphatic C–H stretching, particularly vibrations associated with methylene and methyl groups. The band at 1457.4 cm^{-1}, with an absorbance of 0.204, may be associated with methylene bending or deformation vibrations. These bands are compatible with lipid-associated or other aliphatic molecular structures in the extract.

The relatively weaker absorbance of these bands compared with the bands at 1576.7 and 1039.9 cm^{-1} suggests that aliphatic structures made a smaller spectral contribution under the experimental conditions. However, this observation does not establish the absolute lipid content of the extract. Differences in absorptivity, molecular environment, sample concentration and overlapping bands may influence the observed absorbance. Therefore, the FTIR data support the possible presence of lipid-associated constituents but do not quantify the lipid fraction. The occurrence of lipid-associated vibrations in an aqueous extract is not unexpected because some amphiphilic molecules, membrane-associated compounds and lipid–protein complexes may be extracted or dispersed in water. Direct quantification of lipids would require an independent analytical method such as gravimetric extraction, gas chromatography or high-performance liquid chromatography.

3.2.3 Carboxylate- and Oxygen-Containing Structures

The band at 1397.8 cm^{-1}, with an absorbance of 0.300, occurs in a region that may include symmetric stretching vibrations of carboxylate groups. Such groups may occur in amino acids, organic acids, fatty-acid-related structures and other oxygen-containing compounds. The assignment is therefore consistent with the possible presence of carboxyl-containing constituents, although overlapping vibrations cannot be excluded.

The band at 1263.6 cm^{-1}, with an absorbance of 0.223, lies in a region that may contain C–O, P–O and other overlapping vibrations. It may be compatible with ester- or phosphate-containing structures, including possible phospholipid-associated components. However, this band alone cannot be regarded as definitive evidence of phospholipids. Confirmation would require lipid-specific extraction and chromatographic or spectrometric characterization. Carboxylate-containing molecules may participate in metal binding, acid–base reactions and other biochemical processes. Some organic acids also possess antioxidant properties. However, the present FTIR spectrum does not establish the identity of the compounds responsible for the 1397.8 cm^{-1} band. The possible occurrence of carboxyl-containing structures is therefore best regarded as a chemical feature that may warrant further investigation.

3.2.4 Carbohydrate-Associated Bands

The bands at 1118.2 and 1039.9 cm^{-1}, with absorbances of 0.304 and 0.380, respectively, are consistent with C–O stretching vibrations commonly observed in carbohydrates, alcohols, ethers and polysaccharide-related structures. The band at 1039.9 cm^{-1} displayed the highest absorbance among the principal bands listed in Table 2, indicating a strong contribution from molecular groups absorbing in this region.

The strong spectral contribution around 1039.9 cm^{-1} is consistent with the known carbohydrate-rich composition of finger millet (Fuller, 2014; Ramashia et al., 2019). However, the absorbance cannot be used alone to determine the precise carbohydrate or polysaccharide concentration. The band may include contributions from several C–O-containing compounds, and its intensity may be influenced by sample preparation and matrix effects. The carbohydrate-associated bands

indicate that sugars, polysaccharides or other oxygenated organic compounds may constitute important components of the aqueous extract. Further analysis using total carbohydrate assays, reducing-sugar assays, chromatographic separation or nuclear magnetic resonance spectroscopy would be required to determine the identity and relative abundance of these compounds.

3.2.5 Aromatic and Phenolic-Associated Bands

The bands at 849.8849.8 and 771.6 cm^{-1}, with absorbances of 0.240 and 0.264, respectively, occur in the fingerprint region. They may involve aromatic C–H bending, out-of-plane deformation or other overlapping skeletal vibrations. Their presence is compatible with aromatic constituents, including the possibility of phenolic or other secondary metabolites. However, the two bands do not conclusively establish the presence of specific phenolic compounds. Phenolic molecules often exhibit several overlapping absorptions, and fingerprint-region bands may be produced by different classes of aromatic and non-aromatic compounds. Consequently, the FTIR results should be interpreted as evidence of possible aromatic structures rather than definitive identification of phenolic antioxidants. Phenolic compounds are of interest in radiation-biology research because some can donate hydrogen atoms or electrons, stabilize radical intermediates and chelate certain metal ions (Jagetia, 2007; Montoro et al., 2023). Nevertheless, the possible presence of aromatic or phenolic structures in the extract does not demonstrate free-radical-scavenging activity. This would require direct assays such as DPPH, ABTS, hydroxyl-radical, superoxide-radical, ferric-reducing antioxidant power or cellular oxidative-stress measurements.

3.2.6 Relative Absorbance Intensities

The relative absorbance intensities of the principal FTIR bands are presented in Fig. 2. The band at 1039.9 cm^{-1} showed the highest absorbance among the principal bands, followed by the bands at 1576.7, 663.5, 1118.2 and 1397.8 cm^{-1}. These differences indicate that carbohydrate- and protein-associated spectral regions made substantial contributions to the measured spectrum. However, the relative intensity of an FTIR band is not a direct measure of the concentration of a particular functional group. It is affected by the molar absorptivity of the vibration, sample thickness, concentration, instrumental conditions, baseline correction and overlapping absorptions.

Accordingly, Fig. 2 is useful for comparing the measured spectral responses, but it should not be interpreted as a quantitative compositional analysis. The FTIR data provide evidence of broad chemical classes, while accurate quantification would require calibration against appropriate standards and independent chemical assays.

3.3 Implications of the Elemental Composition for Possible Radioprotective Activity

The NAA results provide a useful basis for discussing the possible biological relevance of the inorganic constituents of *E. coracana* seed extract. Radiation-induced biological damage is associated with direct energy deposition and indirect oxidative processes involving reactive oxygen species. The indirect pathway is particularly important in aqueous biological systems because ionizing radiation can produce reactive species through water radiolysis. These species may subsequently react with lipids, proteins, carbohydrates and nucleic acids.The elemental profile indicates the presence of zinc, iron, potassium, sodium and other mineral constituents that participate in normal biological processes. However, the measured concentrations should be interpreted as compositional data rather than direct evidence of radioprotective efficacy.

3.3.1 Zinc

Zinc was detected at 55±4.2955 mg/kg. Zinc is an essential trace element associated with the structure and function of numerous proteins and enzymes. It is a component of Cu/Zn-SOD, which catalyses the conversion of superoxide radicals into hydrogen peroxide and molecular oxygen (Prasad, 2013). Zinc is also involved in protein stabilization, cellular signalling and the function of some DNA-associated proteins (Hambidge, 2000; Shils et al., 2006). These functions provide a reasonable basis for investigating whether zinc-containing constituents of the extract contribute to antioxidant or cellular-protective effects.

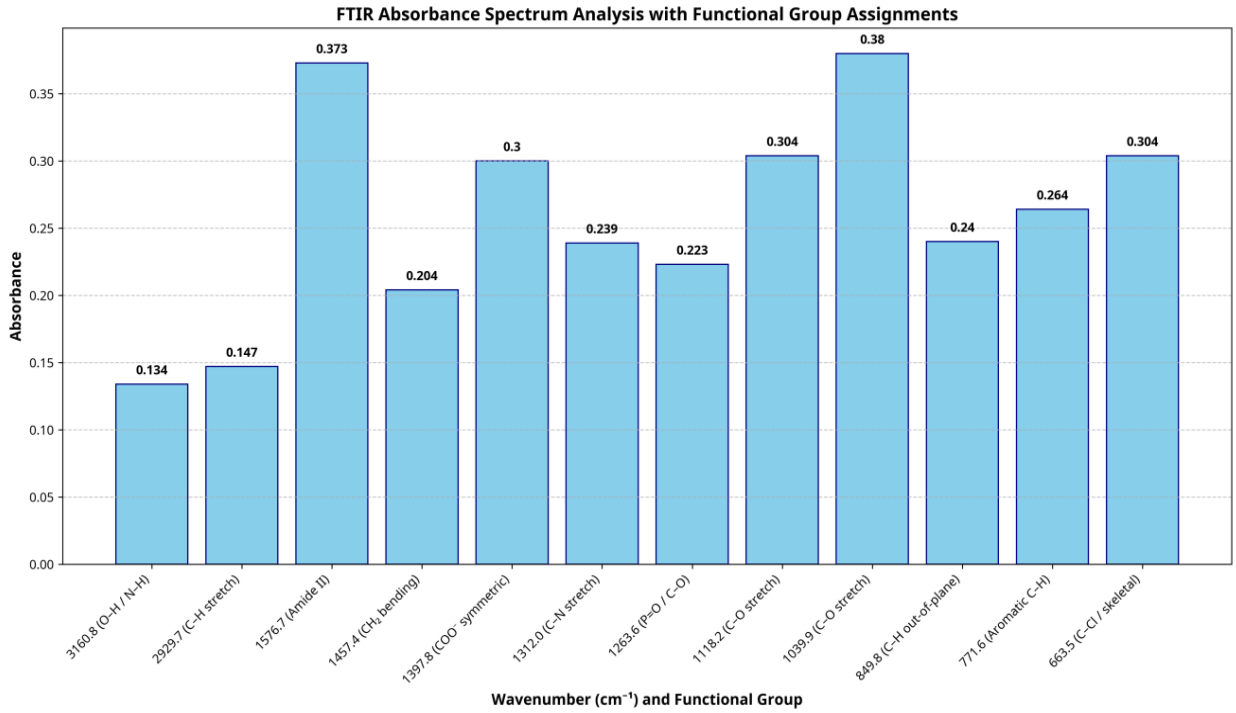

Fig/ 2. Relative absorbance intensities of the principal FTIR bands identified in the Eleusine coracana seed extract

Nevertheless, the detection of zinc does not demonstrate that the extract contains active SOD, increases SOD activity or protects cells from radiation. In addition, zinc may be present in several chemical forms, and its bioavailability cannot be determined from NAA. Direct measurements of SOD activity, intracellular zinc status and oxidative-stress biomarkers would be required to establish a functional relationship.

3.3.2 Iron

Iron was detected at 33±3 mg/kg. Iron is required for oxygen transport, electron-transfer reactions and the activity of several enzymes. It is also associated with catalase and peroxidase systems. However, free or poorly controlled redox-active iron can participate in Fenton-type reactions and contribute to hydroxyl-radical formation (Underwood, 1977). This dual role is important in interpreting the possible radioprotective relevance of the extract. Iron may support normal metabolism when appropriately regulated, but excess or improperly coordinated iron may intensify oxidative damage. The present results do not provide information about the oxidation state, ligand environment, solubility or bioavailability of the detected iron. Therefore, it would be inappropriate to conclude that the

measured iron concentration enhances catalase or peroxidase activity. Iron-related effects should be investigated through metal-speciation studies, oxidative-stress assays and biological experiments.

3.3.3 Potassium and Sodium

Potassium and sodium were detected at 15,460±62 and 219±1 mg/kg, respectively. These elements are essential electrolytes involved in osmotic regulation, membrane potential, nutrient transport and cellular homeostasis. Disturbances in ion balance may contribute to cellular dysfunction during severe oxidative or radiation-induced stress. The high potassium concentration indicates that the extract may be a substantial source of potassium on a mass basis. However, the concentration measured in the extract does not directly establish the amount that would be absorbed or physiologically available after administration. Furthermore, potassium concentration alone cannot demonstrate membrane stabilization or protection against radiation-induced cell death. The potential relevance of these electrolytes is therefore nutritional and physiological rather than direct evidence of radioprotection.

3.3.4 Selenium

Selenium is commonly associated with glutathione peroxidase and other selenoproteins involved in the regulation of oxidative stress (Chandra, 1997). However, selenium was not included as a separate entry in the supplied NAA table. Consequently, the available results do not permit a definitive conclusion regarding its concentration or absence in the extract. If selenium was measured and found to be below the detection limit, it should be added to Table 1 with its corresponding detection limit and reported as BDL. Otherwise, discussion of selenium should remain limited to its general biological importance and should not be presented as a measured characteristic of the present extract.

3.3.5 Other Trace and Rare Elements

The extract contained low concentrations of La, Sm, Sc, Co, Cs, Eu, Tb and Th. Their detection indicates the complexity of the mineral composition of the plant material. However, these elements should not be automatically classified as beneficial or radioprotective. Their biological effects depend on concentration, chemical form, exposure route and toxicological properties. The present NAA results do not provide sufficient evidence to assign a protective function to these elements. The results also highlight the importance of evaluating the safety of plant extracts intended for biological applications. In addition to determining potentially beneficial minerals, future investigations should assess elemental speciation, permissible exposure levels and possible accumulation of less familiar trace elements.

3.3.6 Overall Interpretation of the NAA Findings

The NAA data indicate that *E. coracana* seed extract contains a mixture of electrolytes, essential micronutrients and low-level trace elements. Zinc and iron are particularly relevant to oxidative-stress biology, while potassium and sodium are important for cellular homeostasis. Nevertheless, the elemental profile alone cannot demonstrate direct radical scavenging, enzyme activation, DNA protection, membrane stabilization or improved survival after irradiation. The NAA results should therefore be regarded as a foundation for further investigation. The biological significance of the detected elements can only be established by integrating elemental measurements with chemical speciation, bioavailability studies, antioxidant assays and radiation-exposure experiments.

3.4 Implications of FTIR-Detected Functional Groups for Possible Radioprotection

The FTIR results identified spectral regions compatible with hydroxyl-, amino-, carbonyl-, carboxyl-, aliphatic and carbohydrate-associated structures. These chemical features may be relevant to the biological activity of the extract because plant-derived molecules can participate in hydrogen donation, electron transfer, metal binding and interactions with biological membranes. However, the FTIR data do not establish the identity, concentration or biological activity of the compounds responsible for the observed bands.

3.4.1 Aromatic and Phenolic-Related Structures

The bands at 849.8849.8849.8 and 771.6 cm^{-1} may be associated with aromatic C–H bending or other fingerprint-region vibrations. If phenolic compounds are present, their hydroxyl groups may contribute to antioxidant activity through hydrogen- or electron-transfer reactions. Some phenolic compounds can also chelate redox-active metals and reduce metal-catalysed oxidative reactions (Jagetia, 2007). Nevertheless, the present FTIR spectrum only indicates that aromatic structures may be present. It does not identify particular phenolic compounds or establish their radical-scavenging capacity. The possible contribution of phenolic constituents to radioprotective activity must therefore be tested using chromatographic identification and direct antioxidant or radiation-biology assays.

3.4.2 Protein- and Peptide-Related Structures

The bands at 1576.71576.7 and 1312.0 cm^{-1} are compatible with protein- or peptide-related structures. Such constituents may influence the chemical behaviour of the extract through metal binding, hydrogen bonding or interactions with other biomolecules. Protein-related components could also contribute amino-acid residues capable of reacting with oxidants. However, the spectrum does not establish the presence of specific antioxidant proteins, DNA-repair proteins or active enzymes. It is also important to distinguish proteins from low-molecular-weight antioxidant systems. Glutathione, for example, is a tripeptide rather than a protein, while thioredoxin is a protein-based redox system. The current FTIR data cannot determine whether either system is present or active. Therefore, the protein-associated bands should be interpreted as evidence of possible nitrogen-containing biomolecular structures requiring further characterization (Barth, 2007; Kong & Yu, 2007).

3.4.3 Carbohydrate and Polysaccharide-Related Structures

The bands at 1118.2 and 1039.9 cm^{-1} are compatible with C–O-containing carbohydrate structures. Plant carbohydrates and polysaccharides may have biological effects through their physicochemical properties, interactions with proteins and possible immunomodulatory activities. Some plant-derived polysaccharides have been investigated for their influence on immune responses and recovery processes following stress (Montoro et al., 2023). However, the presence of a strong carbohydrate-associated FTIR band does not establish that the extract contains biologically active polysaccharides or that these compounds enhance hematopoietic recovery after irradiation. Nor does it demonstrate that carbohydrates absorb radiation energy in a sacrificial protective mechanism. Such claims would require direct experimental evidence. The present findings only justify further investigation of the carbohydrate fraction using carbohydrate quantification, molecular-weight analysis and biological assays.

3.4.4 Possible Phosphate- and Ester-Containing Structures

The band at 1263.6 cm^{-1} occurs in a region that may include C–O, P–O and other overlapping vibrations. It may therefore be compatible with ester- or phosphate-containing compounds. If phospholipid-associated molecules are present, they could be relevant to membrane-related processes because membrane lipids are

susceptible to oxidative damage during radiation exposure. However, the band does not independently confirm phospholipids or demonstrate membrane stabilization. Lipid peroxidation, membrane leakage and changes in membrane fluidity would need to be measured directly to establish whether the extract protects biological membranes (Kiang & Olabisi, 2019).

3.4.5 Carboxyl-Containing Structures

The band at 1397.8 cm^{-1} may involve carboxylate-associated vibrations. Carboxyl-containing compounds occur in amino acids, fatty acids and organic acids. Some of these compounds can participate in metal binding or antioxidant reactions. For example, certain organic acids may influence the availability of transition metals and thereby affect oxidative reactions (Arora, 2008). Nevertheless, the FTIR result does not identify the particular carboxyl-containing molecules in the extract. The observed band should therefore be considered a tentative indication of carboxylate-related chemistry rather than proof of a specific antioxidant compound.

3.5 Integrated Interpretation of the NAA and FTIR Findings

The integration of NAA and FTIR data provides a broader chemical description of *E. coracana* seed extract than either method could provide alone. NAA identified the inorganic constituents, particularly potassium, rubidium, sodium, zinc, iron, bromine and several trace elements. FTIR indicated the presence of molecular environments compatible with carbohydrates, protein- or peptide-related structures, aliphatic compounds, carboxyl-containing molecules and possible aromatic constituents. These findings support the view that the extract is chemically complex and contains both mineral and organic components. The chemical complexity provides a basis for proposing possible biological activities, but it does not establish a radioprotective effect. The proposed framework should therefore be considered a hypothesis-generating interpretation rather than a demonstrated mechanism.

3.5.1 Possible Radical-Scavenging Activity

The aromatic fingerprint-region bands may be compatible with phenolic or other aromatic constituents, while the carbohydrate-associated bands indicate the presence of C–O-rich molecules. If phenolic compounds are present, they may contribute to antioxidant activity through hydrogen- or electron-transfer reactions (Jagetia, 2007). However, the FTIR bands do not establish the concentration or activity of such compounds.

Similarly, carbohydrates should not automatically be regarded as direct radical scavengers. The possible antioxidant activity of the extract must be established using chemical assays and, preferably, biological models that measure reactive oxygen species and oxidative damage.

3.5.2 Possible Support of Antioxidant Enzyme Systems

The detection of zinc and iron provides a biochemical rationale for examining the extract's relationship with antioxidant enzymes. Zinc is associated with Cu/Zn-SOD, while iron is involved in several essential enzymes, including catalase-related systems (Prasad, 2013; Underwood, 1977). However, mineral detection does not prove that the extract contains the active enzymes, that the minerals are bioavailable or that enzyme activity is enhanced.

The appropriate interpretation is that the elemental profile identifies constituents that may be relevant to antioxidant physiology. Future studies should measure SOD, catalase, glutathione peroxidase, glutathione reductase and related biomarkers directly.

3.5.3 Possible Membrane-Related Effects

The bands at 2929.7 and 1457.4 cm^{-1} indicate possible aliphatic or lipid-associated structures, while the band at 1263.6 cm^{-1} may involve C–O- or P–O-containing compounds. These spectral features may justify further

investigation of membrane-related effects. Radiation-induced oxidative damage can involve lipid peroxidation and disruption of membrane permeability (Kiang & Olabisi, 2019). However, the current results do not demonstrate that the extract contains membrane-stabilizing phospholipids or prevents lipid peroxidation. Such a conclusion would require measurements of malondialdehyde, lipid hydroperoxides, membrane leakage, membrane fluidity or cell viability following irradiation.

3.5.4 Possible DNA-Protective Relevance

Zinc is associated with several DNA-related proteins and cellular regulatory processes (Hambidge, 2000). In addition, antioxidant molecules may indirectly reduce DNA damage by decreasing the concentration of reactive species. However, neither the zinc concentration nor the protein-associated FTIR bands demonstrates DNA protection or DNA-repair activity. Direct assessment would require assays such as comet analysis, micronucleus testing, γ-H2AX measurement, DNA fragmentation analysis or other validated genotoxicity and radioprotection methods. The present findings therefore provide only a rationale for future DNA-protection studies.

3.5.5 Possible Immunomodulatory Relevance

The carbohydrate-associated FTIR bands suggest the presence of carbohydrate-rich constituents, and some plant polysaccharides have been investigated for immunomodulatory effects (Montoro et al., 2023). However, the present spectrum does not establish the presence of biologically active polysaccharides, their molecular weights or their effects on immune cells. Consequently, the possibility of immunomodulatory activity should be regarded as a testable hypothesis. Confirmation would require polysaccharide isolation, structural characterization and biological evaluation using appropriate immune or hematopoietic models.

3.6 Proposed Radioprotective Framework

Based on the combined NAA and FTIR findings, *E. coracana* seed extract may contain chemical constituents relevant to several pathways involved in oxidative stress. These pathways are presented below as possible mechanisms requiring experimental validation.

1. Direct antioxidant activity: Possible aromatic or phenolic constituents may contribute to radical-scavenging activity if they are present in sufficient concentrations and possess suitable chemical structures (Jagetia, 2007).
2. Metal-associated antioxidant processes: Zinc and iron may be relevant to antioxidant physiology, although their effects depend on chemical form, bioavailability and biological regulation (Prasad, 2013; Underwood, 1977).
3. Membrane-related effects: Aliphatic and possible ester- or phosphate-containing structures may justify investigation of lipid peroxidation and membrane integrity. The FTIR spectrum alone does not prove membrane stabilization.
4. DNA protection: The presence of zinc and possible protein-related structures provides a rationale for studying DNA damage and repair, but no DNA-protective effect was demonstrated in the present work (Hambidge, 2000).
5. Immune and cellular recovery: Carbohydrate-associated constituents may warrant investigation for possible immunomodulatory effects, but the current data do not establish immune stimulation or hematopoietic recovery (Montoro et al., 2023).

The proposed framework is therefore preliminary. It links the chemical features detected by NAA and FTIR with biological processes that may be relevant to radiation-induced damage. Direct evidence of radioprotection would require controlled irradiation experiments involving appropriate

positive and negative controls, dose–response analysis and validated biological endpoints.

3.7 Interpretation of FTIR Absorbance and Photon Energy

The FTIR spectrum can be interpreted in relation to infrared photon energy using the relationship between photon energy and wavenumber:

$$E = hc\bar{\nu} \quad (9)$$

where EEE is the photon energy, hhh is Planck's constant, ccc is the speed of light and ν~\tilde{\nu}ν~ is the wavenumber. The calculated energy for the band at 1039.9 cm^{-1} is approximately 2.066×10^{-20} J per photon, whereas the band at 1576.7 cm^{-1} corresponds to approximately 3.132×10^{-20} J per photon. These values describe the energies of infrared photons associated with the measured vibrational frequencies. The calculated photon energies should not be interpreted as bond-dissociation energies, energies required to break chemical bonds or direct measures of radiation-induced biological damage. FTIR absorption involves excitation of molecular vibrational modes, and the observed bands reflect the interaction of infrared radiation with functional groups in the sample.

The strongest band in the measured spectrum occurred at 1039.9 cm^{-1}, with an absorbance of 0.380. The band at 1576.7 cm^{-1} had an absorbance of 0.373. These values indicate strong relative spectral responses under the experimental conditions. However, absolute concentrations cannot be calculated from the absorbance values because the molar absorptivity, optical path length, sample concentration and independent functional-group concentrations were not determined. The absorbance values should therefore be used for comparative interpretation only.

The measured wavenumber range falls within the mid-infrared region. The broader interval of 400040004000–400400400 cm^{-1} corresponds approximately to 0.05 – 0.50 eV per photon. These energies are generally lower than those associated with electronic excitation, which commonly occurs in the approximate range of 1–10 eV, and are far below the energies of ionizing radiation, which may occur in the keV-to-MeV range. This distinction is important because FTIR measures molecular vibrational responses, whereas ionizing radiation can produce ionization, radical formation and extensive chemical damage.

The calculated photon energies therefore strengthen the physical interpretation of the FTIR spectrum but do not establish a radioprotective mechanism. The relevance of the extract to radiation protection must be determined through direct measurements of antioxidant activity, cellular viability, DNA integrity, lipid peroxidation and other radiation-response endpoints.

The combined NAA and FTIR results show that *E. coracana* seed extract contains a diverse mixture of inorganic and organic constituents. Potassium was the predominant detected element, while zinc, iron, sodium, rubidium, bromine and other trace elements contributed to the elemental profile. The FTIR spectrum displayed bands compatible with carbohydrate-rich structures, protein- or peptide-related groups, aliphatic compounds, carboxyl-containing molecules and possible aromatic constituents. The results are important because both mineral nutrients and plant-derived organic compounds may influence biological responses to oxidative stress. Zinc is relevant to antioxidant and DNA-associated processes, iron is essential but may also participate in pro-oxidant reactions, and carbohydrate- or aromatic-containing constituents may possess biological activities depending on their structures and concentrations. Nevertheless, the present analytical methods do not establish the bioavailability, activity or safety of these constituents.

The evidence therefore supports the description of *E. coracana* seed extract as a chemically complex plant-derived material with potential for further radioprotective investigation, rather than as a confirmed radioprotective agent. The

proposed mechanisms involving radical scavenging, antioxidant enzyme support, membrane protection, DNA protection and immune modulation remain hypotheses. They require validation through antioxidant assays, enzyme-activity measurements, chemical profiling, cellular studies, DNA-damage assays, animal experiments and controlled irradiation studies. The principal limitation of the present analysis is that it was based on elemental and FTIR characterization. These techniques provide valuable chemical information but do not directly measure radioprotective efficacy. Further studies should therefore establish the extract's phytochemical composition, antioxidant capacity, cytotoxicity, dose response, cellular uptake and ability to reduce radiation-induced biochemical and genetic damage.

4.0 Conclusion

This study successfully characterized an aqueous extract of *Eleusine coracana* seeds using NAA and FTIR spectroscopy, providing the first comprehensive report of its elemental and functional group composition. NAA revealed a diverse elemental profile dominated by potassium (15460 ± 62 mg/kg), with significant quantities of zinc (55 ± 4.29 mg/kg), iron (33 ± 3 mg/kg), rubidium (364 ± 9 mg/kg), sodium (219 ± 1 mg/kg), and other trace elements (Br, La, Sm, Sc, Cr, Co, Cs, Ba, Eu, Tb, Th) at varying concentrations. Arsenic, uranium, and antimony were below detection limits, indicating the absence of these toxic elements.

FTIR analysis identified absorption bands associated with protein (amide I and II, 1576.7 cm^{-1} and 1312.0 cm^{-1}), lipid (C–H stretch, 2929.7 cm^{-1} and 1457.4 cm^{-1}), carboxylate (1397.8 cm^{-1}), phospholipid (1263.6 cm^{-1}), carbohydrate (1039.9 cm^{-1} and 1118.2 cm^{-1}), and aromatic (849.8 cm^{-1} and 771.6 cm^{-1}) molecular structures. The strong carbohydrate signature at 1039.9 cm^{-1} (absorbance 0.380) and the amide II band at 1576.7 cm^{-1} (absorbance 0.373) were the most prominent features of the spectrum.

The integration of NAA and FTIR data allows the formulation of a mechanistic framework for the potential radio protective activity of the extract. The phenolic compounds (indicated by aromatic C–H bands) provide direct radical-scavenging capacity, while zinc and iron (detected by NAA) support enzymatic antioxidant defenses. Carbohydrate and phospholipid components contribute to membrane stabilization and immune modulation, and proteinaceous components may participate in DNA repair processes. This multifaceted approach to radioprotection—targeting multiple pathways of radiation damage—represents a significant advantage of natural product extracts over single-compound synthetic radio protectors.

The theoretical treatment using photon-energy relations, wavenumber and the Beer–Lambert law provides a clear physical basis for interpreting the observed spectral features. The calculated photon energies for the absorption bands range from 0.082 to 0.392 eV, confirming that the observed absorptions correspond to vibrational excitations of molecular bonds.

The findings demonstrate the chemical richness of *E. coracana* and support its consideration as a candidate for further investigation of natural radio protective agents. However, the present study is a characterization study; direct radio protective efficacy cannot be established from NAA and FTIR characterization alone and requires subsequent biological and irradiation studies. The comprehensive characterization provided here establishes essential baseline data for these future investigations.

Future investigations should include biological studies to evaluate the radio protective efficacy suggested by the chemical characterization presented in this paper.

Acknowledgement
The authors are grateful to the Department of Physics, Bayero University Kano, and Ahmadu Bello University, Zaria, for supporting the research with laboratory facilities and technical assistance.

5.0 References

Agarwal, K. N. (2001). Trace elements in human nutrition and health. World Health Organization.

Arora, R. (2008). Herbal radioprotectors: Applications and mechanisms. CABI Publishing.

Arora, R., Gupta, D., Chawla, R., Sagar, R., Sharma, A., Kumar, R., … Sharma, R. K. (2005). Radioprotection by plant products: Present status and future prospects. Phototherapy Research, 19(1), pp. 1–22.

Arzoo, Neeru, Shukla, A. K., Panwar, S., & Kumar, A. (2024). Effect of processing techniques on functional, antioxidants, and structural properties of finger millet (Eleusine coracana) flour. Food and Humanity, 2, Article 100305. https://doi.org/10.1016/j.foohum.2024.100305

Bagheri, R., Gholami, M., & Mohammadi, A. (2018). Radiation applications and biological effects: A review. Radiation Physics and Chemistry, 144, pp. 1–8.

Barth, A. (2007). Infrared spectroscopy of proteins. Biochimica et Biophysica Acta—Bioenergetics, 1767(9), pp. 1073–1101.

Bode, P. (1996). Automation and quality assurance in neutron activation analysis. Journal of Radioanalytical and Nuclear Chemistry, 204(2), pp. 257–267.

Chai, Y., Liu, X., & Zhang, H. (2020). Radiation exposure and associated risks in modern environments. Environmental Research, 182, pp. 109–118.

Chandra, R. K. (1997). Nutrition and the immune system: An introduction. The American Journal of Clinical Nutrition, 66(2), pp. 460S–463S.

Cember, H. (1969). Introduction to health physics. Pergamon Press.

Currie, L. A. (1968). Limits for qualitative detection and quantitative determination. Analytical Chemistry, 40(3), pp. 586–593.

Das, S., Roy, P., & Chakraborty, S. (2024). Application of neutron activation analysis in material characterization. Journal of Radioanalytical and Nuclear Chemistry, 331(1), pp. 45–56.

Desouky, O., Ding, N., & Zhou, G. (2015). Targeted and non-targeted effects of ionizing radiation. Journal of Radiation Research and Applied Sciences, 8(2), pp. 247–254.

Dowlath, M. J., Karuppannan, S., & Suresh, S. (2021). Radiation-induced oxidative stress and biological damage: Mechanisms and protection strategies. Environmental Science and Pollution Research, 28(12), pp. 14530–14544.

Ehmann, W. D., & Vance, D. E. (1991). Radiochemistry and nuclear methods of analysis. Wiley.

Firestone, R. B., & Shirley, V. S. (1996). Table of isotopes (8th ed.). Wiley-Interscience.

Fuller, D. Q. (2014). Finger millet: A forgotten crop with high nutritional value. Journal of Agricultural Science, 6(8), pp. 1–12.

Gillette, E. L., & Alpen, E. L. (1998). Radiation biology and its applications in medicine. Radiation Research, 150(5), pp. S1–S6.

Glascock, M. D. (2004). Neutron activation analysis and its applications in archaeology. Measurement Science and Technology, 15(3), pp. 1–9.

Greenberg, R. R., Bode, P., & De Nadai Fernandes, E. A. (2011). Neutron activation analysis: A primary method of measurement. Spectrochimica Acta Part B: Atomic Spectroscopy, 66(3–4), pp. 193–241.

Haghparast, A., et al. (2017). FTIR spectroscopy applications in biochemical analysis. Spectrochimica Acta Part A:

Molecular and Biomolecular Spectroscopy, 178, pp. 1–10.

Hambidge, M. (2000). Human zinc deficiency. The Journal of Nutrition, 130(5), pp. 1344S–1349S.

Hassan, Z., Ahmad, S., & Khan, R. (2021). Nutritional and health benefits of millet consumption. Food Science & Nutrition, 9(3), pp. 1503–1512.

Hosseinimehr, S. J. (2007). Trends in the development of radioprotective agents. Drug Discovery Today, 12(19–20), pp. 794–805.

Ibrahim, A. M., Forsido, S. F., & Kuyu, C. G. (2024). Nutritional quality and functional properties of finger millet, sweet potato, and soybean composite flour as affected by blending ratios. Discover Food, 4(1), Article 135. https://doi.org/10.1007/s44187-024-00212-6

Ila, P., & Jagam, P. (1980). Multielement analysis of biological materials by neutron activation analysis. Journal of Radioanalytical Chemistry, 57(1), pp. 205–218.

International Commission on Radiological Protection. (1991). 1990 recommendations of the International Commission on Radiological Protection (ICRP Publication 60). Pergamon Press.

Jagetia, G. C. (2007). Radioprotective effects of plants and herbs. Journal of Clinical Biochemistry and Nutrition, 40(2), pp. 74–81.

Jagetia, G. C., & Baliga, M. S. (2005). The evaluation of radioprotective effects of herbal extracts. Phototherapy Research, 19(10), pp. 1–10.

Jit, S., et al. (2022). Natural radioprotectors and their mechanisms. Journal of Radiation Research, 63(2), pp. 1–12.

Kiang, J. G., & Olabisi, A. O. (2019). Radiation: A poly-traumatic hit leading to multi-organ injury. Cell & Bioscience, 9(1), pp. 1–15.

Kokisi, P., Nchu, F., Kambizi, L., & Bvenura, C. (2026). Finger millet and soybean as functional ingredients in next-generation fermented foods: A review of nutritional, technological, and health-promoting perspectives. Frontiers in Nutrition, 13, Article 1718090. https://doi.org/10.3389/fnut.2026.1718090

Kong, J., & Yu, S. (2007). Fourier transform infrared spectroscopic analysis of protein secondary structures. Acta Biochimica et Biophysica Sinica, 39(8), pp. 549–559.

Landsberger, S. (2006). Activation analysis in environmental studies. Journal of Radioanalytical and Nuclear Chemistry, 267(3), pp. 1–10.

Magill, J., Pfennig, G., & Galy, J. (2006). Karlsruher nuklidkarte (7th ed.). European Commission Joint Research Centre.

Montoro, A., et al. (2023). Natural compounds as radioprotective agents. Antioxidants, 12(1), pp. 1–15.

Nair, C. K. K., Parida, D. K., & Nomura, T. (2001). Radioprotectors in radiotherapy. Journal of Radiation Research, 42(1), pp. 21–37.

Nandiyanto, A. B. D., Oktiani, R., & Ragadhita, R. (2019). How to read and interpret FTIR spectroscope of organic material. Indonesian Journal of Science and Technology, 4(1), pp. 97–118.

Nilsson, R., & Liu, Y. (2020). Radiation chemistry fundamentals. Radiation Physics and Chemistry, 170, pp. 108–115.

Parke, D. V., & Parke, A. L. (2020). Toxicological mechanisms of radiation exposure. Toxicology Letters, 330, pp. 1–10.

Prasad, A. S. (2013). Discovery of human zinc deficiency: Its impact on human health. Nutrition, 29(6), pp. 1–10.

Ramashia, S. E., Gwata, E. T., & Meddows-Taylor, S. (2019). Nutritional composition and health benefits of finger millet. Journal

of Food Composition and Analysis, 80, pp. 1–10.

Rangacharyulu, C. (2013). Radiation physics and dosimetry. Journal of Medical Physics, 38(1), pp. 1–5.

Shils, M. E., Shike, M., Ross, A. C., Caballero, B., & Cousins, R. J. (2006). Modern nutrition in health and disease (10th ed.). Lippincott Williams & Wilkins.

Smith, B. C. (2018). Fundamentals of Fourier transform infrared spectroscopy (2nd ed.). CRC Press.

Stone, H. B., Coleman, C. N., Anscher, M. S., & McBride, W. H. (2003). Effects of radiation on normal tissue: Consequences and mechanisms. The Lancet Oncology, 4(9), pp. 529–536.

Stuart, B. (2004). Infrared spectroscopy: Fundamentals and applications. Wiley.

Talapko, J., Skrlec, I., Alebić, T., Jukić, M., & Včev, A. (2024). Ionizing radiation: Effects on human health and environment. International Journal of Environmental Research and Public Health, 21(2), pp. 1–15.

Tekin, H. O., Singh, V. P., & Manici, T. (2018). Investigation of gamma-ray shielding properties of materials. Applied Physics A, 124(1), pp. 1–11.

Underwood, E. J. (1977). Trace elements in human and animal nutrition (4th ed.). Academic Press.

Vasquez, C., et al. (2016). Finger millet (Eleusine coracana) as a source of phytochemicals and bioactive compounds. Journal of Food Science, 81(6), pp. R1332–R1341.

Declarations

Funding

The Tertiary Education Trust Fund (TETFund), Nigeria, provided financial support for the 2025 Intervention program of the Institutional Based Research (IBR). The authors acknowledged this assistance.

Ethical Approval

Not applicable

Informed Consent

Not applicable.

Consent for Publication

Not applicable.

Declaration of Competing Interests

The authors declared no competing interests

Data Availability Statement

Data shall be made available upon request**of Interest**

The authors declared no conflict of intere

Author Contributions

Sadauki, H. F. conceptualized the study, coordinated sample preparation, conducted the FTIR and NAA analyses, interpreted the results, and drafted the manuscript. Koki, F. contributed to experimental procedures, data analysis, literature review, and critical revision. Tijjani, S. F. supported methodological development, interpretation of findings, manuscript editing, and technical validation. All authors reviewed and approved the final manuscript.